EEG Sensorimotor Correlates of Speed During Forearm Passive Movements

Fumiaki Iwane, Giuseppe Lisi, and Jun Morimoto

***Abstract*— Although passive movement therapy has been widely adopted to recover lost motor functions of impaired body parts, the underlying neural mechanisms are still unclear. In this context, fully understanding how the proprioceptive input modulates the brain activity may provide valuable insights. Specifically, it has not been investigated how the speed of motions, passively guided by a haptic device, affects the sensorimotor rhythms (SMR). On the grounds that faster passive motions elicit larger quantity of afferent input, we hypothesize a proportional relationship between localized SMR features and passive movement speed. To address this hypothesis, we conducted an experiment where healthy subjects received passive forearm oscillations at different speed levels while their electroencephalogram was recorded. The mu and beta event related desynchronization (ERD) and beta rebound of both left and right sensorimotor areas are analyzed by linear mixed-effects models. Results indicate that passive movement speed is correlated with the contralateral beta rebound and ipsilateral mu ERD. The former has been previously linked with the processing of proprioceptive afferent input quantity, while the latter with speed-dependent inhibitory processes. This suggests the existence of functionally-distinct frequency-specific neuronal populations associated with passive movements. In future, our findings may guide the design of novel rehabilitation paradigms.**

***Index Terms*— Electroencephalography (EEG), sensorimotor rhythms (SMR), event-related desynchronization (ERD), beta rebound, passive movement speed.**

I. Introduction

In motor rehabilitation, passive movements are typically provided by either a therapist or an assistive device [1], [2]. A growing literature suggests that proprioceptive feedback given to impaired body parts upon the detection of sensorimotor activity promotes plasticity during motor rehabilitation [3]–[6]. The assisted movement produces sensory and proprioceptive afferent input that is hypothesized to induce central nervous system plasticity during Brain Computer Interface rehabilitation, leading to the restoration of normal motor control [7], [8]. Investigating how proprioceptive input is encoded and elaborated by the central nervous system is important for understanding both the physiology of motor control, and the neural mechanisms of motor rehabilitation. Especially, elucidating how sensorimotor rhythms (SMR) are modulated by passive movements may provide additional insights for more effective therapies. Fig. 1 shows our experimental setup for this investigation.

Mechanoreceptors in muscles and joints convey information about posture and movements of the body and thereby play an important role in proprioception and motor control [9]. One of the important receptors for proprioceptive input is the muscle spindle located within skeletal muscles. It plays a crucial role in encoding the effects of the amplitude and speed of body parts as they fire trains of action potentials during muscle stretch that vary as a function of muscle length and velocity [10], [11]. Sensory input captured by the muscle spindle enters the central nervous system through the dorsal root ganglion cells. The somatosensory information flows through the medial lemniscus afferent pathways, leading to the excitation of the somatosensory cortex [9].

Studies on monkeys and cats demonstrate that the primary motor cortex receives proprioceptive afferent input via direct thalamocortical connections [12], [13], via the primary somatosensory cortex and via the secondary somatosensory cortex [14]–[16]. In humans, electroencephalography (EEG) [17]–[19] and magnetoencephalography (MEG) [20]–[22] studies confirm that the human sensorimotor cortex is active during passive movements.

Sensorimotor activity is observed in the form of an event-related (de) synchronization (ERD/ERS). An ERD is a power decrease of mu (10-18 Hz) and beta (18-30 Hz) rhythms that occur in the sensorimotor areas during a motor-related task. A post-movement beta ERS is a power increase following the end of the motor task, typically called beta rebound. The beta rebound (beta ERS) after limb movement is a well known phenomenon; however, the mu ERS is not as widely reported in literature [23]. Moreover, in our preliminary visual inspection of the EEG spectrogram we could not observe a mu ERS (Fig. 2). For all the reasons above, we decided to omit the mu ERS from further analysis. The ERD and beta

Manuscript received October 19, 2018; revised April 9, 2019 and July 5, 2019; accepted August 5, 2019. Date of publication August 12, 2019; date of current version September 6, 2019. This work was supported by the ImPACT Program of Council for Science, Technology and Innovation (Cabinet Office, Government of Japan). It is also based on results obtained from projects commissioned by the New Energy and Industrial Technology Development Organization (NEDO), by the National Institute of Information and Communications Technology (NICT) Japan, and by the Strategic Research Program for Brain Sciences from Japan Agency for Medical Research and development, AMED. *(Fumiaki Iwane and Giuseppe Lisi contributed equally to this work.) (Corresponding author: Giuseppe Lisi.)*

F. Iwane is with ATR Computational Neuroscience Laboratories, Department of Brain Robot Interface, Kyoto 619-0288, Japan, and also with the Defitech Chair in Brain-Machine Interface, École Polytechnique Fédérale de Lausanne, 1202 Genève, Switzerland.

G. Lisi is with ATR Computational Neuroscience Laboratories, Department of Brain Robot Interface, Kyoto 619-0288, Japan, and also with the Nagoya Institute of Technology, Nagoya 466-855, Japan (e-mail: glisi@atr.jp).

J. Morimoto is with ATR Computational Neuroscience Laboratories, Department of Brain Robot Interface, Kyoto 619-0288, Japan.

Digital Object Identifier 10.1109/TNSRE.2019.2934231

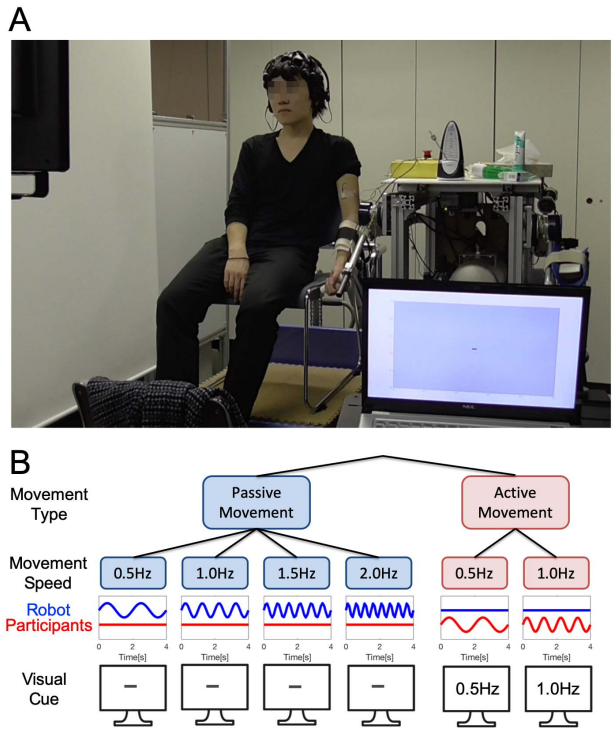

Fig. 1. Experimental protocol. (A) The subject's left forearm is fastened to the robot link while his EEG signal is collected. (B) The experiment is structured as a two-level nested design. The first level consists of movement types, i.e. passive movements (PM) and active movements (AM). The second level represents movement speed, i.e. 0.5 Hz, 1.0 Hz for both PM and AM, and 1.5 Hz, 2.0 Hz only for PM.

rebound are typically associated with cortical activation and deactivation, respectively [24], [25]. Accumulating evidence suggests that the speed of *active movements* is correlated with SMR amplitude [26], [27]. Yuan *et al.* [28] shows that mu and beta ERD power is bilaterally proportional to *active and imagined* hand clenching speed.

Passive movements elicit bilateral mu and beta ERD, and predominantly contralateral beta rebound [18], [19], [29], [30], however the relationship between passive movement speed (i.e. frequency of periodic limb oscillations) and SMR has not been investigated yet. In this study, we designed an EEG experiment to assess whether SMR and the speed of forearm passive oscillations are correlated. Throughout the manuscript we will refer to the frequency (Hz) of periodic limb oscillation as 'speed', in order to avoid any confusion that may arise with the EEG frequency.

Although previous literature has not paid attention to the relationship between SMR and passive movement speed, several studies have shown that SMR power and quantity of afferent input are correlated. These studies are relevant if we consider that faster passive movements elicit a larger quantity of afferent input [22], [31]–[33]. Stancák *et al.* [33] shows that the magnitude of SMR is modulated by intensity of electrical stimuli. Houdayer *et al.* [32] found that voluntary movement and mixed-nerve stimulation elicit a stronger beta rebound than pure tactile stimulation. Parkkonen *et al.* [22] shows that passive movements elicit a stronger and more robust beta rebound than tactile stimulation. This suggests that proprioceptive afferent input elicits a stronger activity than tactile one, and that such activity depends on the type and quantity of the afferent input. Indeed, tactile stimulation activates mainly exteroceptive afferents, whereas passive movements activate primarily proprioceptors and to a lesser extent exteroceptors [22]. Moreover, even though the bilateral beta rebound amplitude correlates with the type and quantity of the afferent input, the ERD is constantly strong bilaterally, across conditions [22], [26], [27]. Therefore, it is hypothesized that the ERD and beta rebound represent frequency-specific anatomically and functionally distinct neural populations.

Based on the cited literature, we hypothesize a proportional relationship between passive movement speed and SMR, only within localized spectral (i.e. mu, beta bands), temporal (i.e. during or post movement) and spatial (i.e. left or right hemisphere) features of the EEG signal.

In order to validate our hypothesis, we designed an experiment where subjects' left forearm was passively moved at four different speed levels. Moreover, since the literature on EEG signals associated with passive movements is somewhat limited compared to that of active movements, we decided to add the active movement condition (at two different speed levels). The active condition would serve as a reference point regarding the excitability induced by active movements of each subject's SMR. As a result, the experiment has a two-level nested design, where the first level is the movement type (i.e. active or passive) and the second level is the movement speed.

II. Materials and Methods

The objective of this work is to investigate the relationship between the magnitude of SMR and speed during forearm passive movement. To this end, we conducted an experiment which is structured as a two-level nested design (i.e. 1st: movement type, 2nd: movement speed), with a forearm exoskeleton robot. In this section, after describing the data acquisition procedure, we explain the data processing to extract SMR features, followed by the statistical analysis of the relationship between SMR and speed.

A. Data Acquisition

To investigate the neural correlates of speed during passive movements, we carried out an experiment with fifteen healthy right-handed subjects aged 23-28 years and without neurological disorders or motor deficits while recording their EEG signals. Besides passive movements, active movements were also taken into consideration in order to set a reference point regarding the excitability induced by active movements of each subject's SMR.

During the experiment, each subject was required to sit on a comfortable chair with the right arm lying relaxed (Fig. 1A). The left elbow was aligned to the joint of a one-degree-of-freedom robot [34], and the left forearm (i.e. non-dominant limb) was fastened to the robot's link. Thanks to the backdrivability of the robot joint (i.e. the robot is able to follow user's induced movements with the least possible resistance), either active or passive movements could be executed while

keeping the forearm fastened to the robot. Indeed, if not actuated, the joint does not oppose any resistance against the subject's motion, except for its gravitational force. During passive movements, subjects were required to relax their muscles, while a sinusoidal elbow movements of the forearm was generated by the robot at a given speed. The angle of the robot joint ranged between -15 to $+15$ degrees with respect to the neutral position. During active movements, the robot was not actuated, and subjects actively performed a similar sinusoidal motion at a given speed. Throughout the experiment, during both the active and passive conditions, subjects were aided with a metronome clicking at 1 Hz. Visual cues were used to give instructions about the speed to produce in the active movement condition.

The experiment is structured as a two-level nested design (Fig. 1B). The first level consists of movement types, i.e. passive movements (PM) and active movements (AM). The second level represents movement speed, i.e. 0.5 Hz, 1.0 Hz for both PM and AM, and 1.5 Hz, 2.0 Hz only for PM. Higher speed levels for either AM or PM were not taken into consideration due to the large muscle and motion artifacts that they would have produced. Therefore, the total number of conditions is 6 (i.e. 4 PM and 2 AM). For each subject, the experiment is composed of 10 sessions interleaved with rest periods of a few minutes. Each session contained 3 trials per condition, resulting in a total of 30 (3×10) trials per condition for a subject. Within a session, conditions were randomized and carried out as follows: an hyphen was shown on the display for 5 s to indicate that the subject should rest. After this period, if the hyphen was maintained, subjects' left forearm was passively moved at either 0.5, 1.0, 1.5 or 2.0 Hz, for the duration of 4 s. Otherwise, if either the cue "0.5 Hz" or "1.0 Hz" appeared on the screen, the subject performed a left forearm sinusoidal active elbow movement at the designated speed for the whole duration of the cue (i.e. 4 s). The spectral analysis of the data, collected by the encoder of the robot, confirms that, on average ($\pm$SD, standard deviation), the speed during active movements matched the target speed with 0.55 ± 0.066 Hz for AM at 0.5 Hz and 0.99 ± 0.08 Hz for AM at 1.0 Hz. The amplitude of motion during active movements was 19.8 ± 5.8 degree for AM at 0.5 Hz and 19.6 ± 4.5 degree for AM at 1.0 Hz. When the robot link is static and parallel to the ground, the gravitational torque generated is 1.34 Nm. An average human forearm (length: 0.46 m, weight: 1.72 kg) in the same condition would generate 3.88 Nm. This means that the weight of the robot only provides additional 34 % of torque due to gravity. Moreover, subjects did not report feeling of resistance due to the additional load. Therefore, we consider that the weight of the robot only have a negligible effect on the active movement condition.

The EEG signal was collected at a sampling rate of 500 Hz by the Quick-20 dry-wireless headset (Cognionics, Inc.), which is a full 10-20 array with 19 channels (F7, Fp1, Fp2, F8, F3, Fz, F4, C3, Cz, P8, P7, Pz, P4, T3, P3, O1, O2, C4, T4) plus reference on A1 and ground on A2 [35]. Moreover, the electromyographic (EMG) signal was acquired from the left-arm biceps, at a sampling rate of 250 Hz, in order to verify that, during passive movements, muscles were not active. Participants gave written informed consent for the experimental procedures, which were approved by the ATR Human Subject Review Committee (Number 16-730).

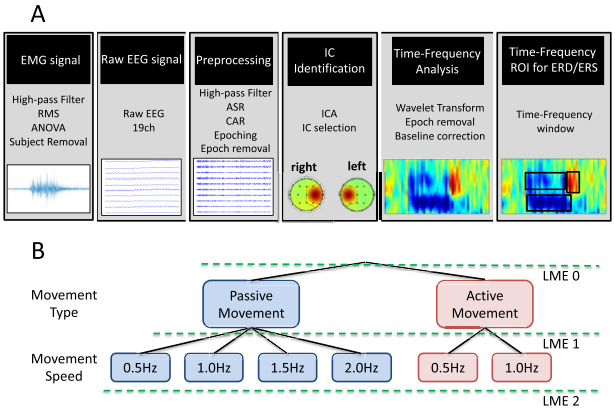

Fig. 2. Data analysis. (A) Signal processing procedure to extract subject-specific SMR power. Mu ERS was not observed after mu ERD in the time-frequency representation (i.e. Time-Frequency ROI for ERD/ERS). Indeed, we do not observe any power increase (i.e. red blob) to the right of the mu ERD (i.e. blue blob at low frequencies). (B) Representation of the linear mixed-effects (LME) nested models used in the statistical analysis.

B. Data Processing

The processing pipeline is visualized in Fig. 2A and it is composed of EMG analysis and EMG-based subject removal, EEG preprocessing, EEG independent component identification, EEG time-frequency analysis and the computation of ERD/ERS amplitudes.

1) EMG Analysis: Before analyzing the EEG signal, we ensure that subjects contract their left-arm biceps during the active conditions, but not in the passive conditions. The root-mean-square (RMS) value of the EMG signal is computed for each trial, after high-pass zero-phase filtering at 10 Hz (4th-order Butterworth) to eliminate low-frequency drift in the signal [36]. The RMS values are computed using the EMG signal recorded during the whole duration of the movement (i.e. 5 s of rest and 4 s of PM/AM), which resulted in one RMS value per trial for a given condition. A one-way ANOVA is performed to evaluate the effect of the movement condition (i.e. rest, PM and AM) on the RMS. As expected, for every subject, we find a significant effect of movement condition ($p < 0.05$). In the subsequent post-hoc t-test analysis, we compare the rest condition with AM and PM, respectively. All subjects exhibit a significant difference ($p < 0.05$) between rest and AM, which confirms that the EMG signal measured the biceps contraction during active movements correctly. Two subjects exhibit a significant difference between rest and PM, indicating that they had been contracting their left-arm biceps during the passive condition. As a result, these two subjects are removed from the subsequent EEG analysis.

2) EEG Preprocessing: Preprocessing consists of high-pass zero-phase filtering by a FIR filter with the cut-off frequency at 1 Hz and the order of 1650 ($3.3 \times sampling frequency$; default parameters computed by EEGLAB), followed by Artifact Subspace Reconstruction (ASR) to remove non-stationary

high-variance signals [37]. After reconstructing the EEG signal from the retained signal subspace, we re-reference it using the common average reference (CAR). Then the signal is segmented into epochs from -2 s to 8 s with respect to movement onset (i.e. 0 s), in order to include the time periods associated with baseline, ERD and post-movement beta rebound.

Subsequently, artifactual epochs are rejected based on established methods [38]. Specifically, we remove epochs with extremely large amplitude (i.e. exceeding -500 or 500 μV), or whose probability of occurrence exceeds a threshold, i.e. 6 SD locally for each channel, and 2 SD globally for all channels regrouped [38]. Thresholds for global and local probability are different because, intuitively, global artifacts are a symptom that the whole epoch is compromised by noise, while local artifacts can be fixed by independent component analysis (i.e. the following step) without throwing the whole epoch away. The amount of epochs rejected per subject is on average 10.5 ± 4.2 (SD) over a total of 180 (i.e. 30 trials per condition).

3) EEG Independent Component Identification: Independent component identification is done by Adaptive Mixture Independent Component Analysis (ICA) [39], in order to decompose different neural and artifactual sources. The input to ICA is the concatenation of post-onset portions of all the retained epochs, which is representative of the movement periods, so to find independent components associated with movement. One independent component per hemisphere, related to left and right SMR respectively, was selected based on visual inspection, using the two criteria described in Wang *et al.* [40]: the spatial pattern should be consistent with the scalp projection of the sensorimotor cortex on each hemisphere; (2) the power spectrum density (PSD) of the component should match the typical spectral profile of mu/beta rhythms. In practice these criteria translate into unilateral spatial distribution (see Fig 2, ICA box) over the sensorimotor cortex (i.e. channels C3 or C4) and a mu/beta-band dominant spectral profile. For each participant, we found exactly two independent components associated with the left and right sensorimotor cortex, respectively.

4) EEG Time-Frequency Analysis: The time-frequency representations of each single-trial EEG independent component are calculated by the Morlet Wavelet transform using EEGLAB with default parameters [41]. The frequency range is set between 7 and 40 Hz, resulting in a wavelet coefficient matrix with 48 time points and 34 linearly-spaced frequency bins. Each of the 48 time windows are composed of 239 samples (478 ms) overlapped by 119 samples (238 ms); while the number of cycles ranges from 3 to 8.57, with an increment of 0.5 from the lowest to the highest frequency. The resulting coefficients are squared to obtain the spectral power.

In addition to the previous epoch rejection, time-frequency representations are also examined for muscle artifacts. Specifically, an epoch is rejected if the power perturbation in the 20 - 40 Hz band deviates by +25 or -100 dB from the baseline (i.e. from -2.0 to -0.5 s.) in either the left or the right independent component [42], [43], which results in the rejection of 8.3 ± 1.6 epochs per subject. The number of remaining epochs, after rejection based on raw amplitude, probability and time-frequency information, is 161.2 ± 3.3.

In order to quantify the magnitude of ERD and beta rebound, we used the baseline correction method proposed in [44]. This approach is less sensitive to noisy trials than classical baseline correction methods, and produces a non-skewed power distribution. In detail, separately for each subject and experimental condition, we apply a single-trial full-epoch baseline correction, before averaging across trials and removing the trial-averaged pre-stimulus (i.e. from -2.0 to -0.5 s.) baseline. It should be noted that the baselines are corrected using the gain model assumption (i.e. divide by the baseline) as opposed to the additive model (i.e. subtract the baseline) [44], and that the trial-averaged pre-stimulus corrected time frequency coefficients are log-transformed ($10log_{10}$) only for visualization purposes.

5) Time-Frequency ROI for ERD and Beta Rebound: SMR patterns are highly subject-specific in frequency and time [45]. Therefore, we used the heuristic introduced in previous literature [45] to automatically define subject-specific time-frequency region of interest (ROI) for mu, beta ERD and post-movement beta rebound. In summary, the algorithm finds the frequency and time ranges of an ROI that maximizes the difference in power between the motor task and baseline. This is accomplished by selecting the ROI ranges for which the correlation coefficient across trials between the class labels (i.e. 0 for baseline and 1 for motor task) and the respective power is above a given threshold. For this purpose, the single-trial squared wavelet coefficients are used.

The algorithm starts by optimizing the frequency range while keeping the default time range (i.e. DTR) fixed: for mu and beta ERD the time ranges are [-2,-0.5] s for class 0 and [0, 4] s for class 1, while for the beta rebound the time ranges are [-2.0, -0.5] s for class 0 and [4, 6] s for class 1. Frequencies with a high correlation coefficient between the time-averaged power and class labels are iteratively added to the optimal frequency band: at first, the frequency with the largest correlation is selected and then the adjacent frequencies (i.e. above and below) are added if their correlation is at least 60% of the best correlation. This search is constrained within [10, 18] Hz for the mu ERD, [18, 30] Hz for the beta ERD and the beta rebound [24], [45].

The same algorithm is executed to optimize the time-domain during the motor task, while keeping the optimal frequency bands previously selected: at first, the time bin with the largest correlation is selected and then the adjacent time bins (i.e. before and after) are added if their correlation is at least 30% of the best correlation. In this case, the threshold for the inclusion of adjacent time bins is lowered (i.e. 30%) because of the higher temporal variability of the ERD. Indeed, the power also has to be smoothed in time with a sliding window [-0.75, 0.75] s, as in the original algorithm [45]. In order to separate the ERD and the beta rebound ROIs, the initial search for the time bin with the largest correlation coefficient is constrained within [0, 4] s for the mu and beta ERD and within [4, 6] s for the beta rebound.

The following criteria have to be fulfilled before ROIs are finally adopted: 1) the frequency range must contain more than

1 frequency bin (i.e. 1 Hz); 2) the ROI duration of mu and beta ERD has to be at least half of the motor task duration (i.e. 2 s); 3) the ROI of beta rebound has to start after the motor task offset (i.e. 4 s), and be longer than half of the corresponding DTR (i.e. 1 s). If an ROI does not meet the aforementioned criteria for a subject, the ranges of that ROI are replaced with those computed using the averaged ranges across valid ROIs of other subjects. If a subject has all invalid ROIs, he/she is rejected from the subsequent statistical analysis. Based on this criterion, 2 subjects are removed, leaving a total of 11 subjects for the following statistical analysis.

In order to compute the mu, beta ERD and beta rebound powers, we take the trial-averaged baseline-corrected power, prior to log-transformation, and average it within a given ROI. Subsequently, this average is log-transformed in order to obtain the relative change in decibel.

C. Statistical Analysis

The statistical modeling of the relationship between SMR, movement types and speed, is carried out by a linear mixed-effects (LME) nested model. For each of the six types of SMR (i.e. mu, beta ERD, beta rebound in both hemisphere) a model is fitted. Models were designed a priori based on the experiment design. According to the Wilkinson notation, the linear mixed-effects model is specified as:

```
SMR = MovType + MovType:Speed + (1| Subject)
```

where the continuous response variable `SMR` is the power of either mu, beta ERD or beta rebound at a given hemisphere, the fixed-effect predictor `Speed` is nested within the variable `MovType`. The random-effect `(1| Subject)` allows for a different intercept per subject. All variables, except `SMR`, are categorical variables. In order to evaluate the effect of `MovType:Speed`, a likelihood ratio test is performed between the previously specified linear mixed model and simpler ones (Fig. 2B), meaning that the following models are tested in a pairwise fashion:

```
LME0: SMR = 1 + (1| Subject)
LME1: SMR = MovType + (1| Subject)
LME2: SMR =
      MovType + MovType:Speed
      + (1| Subject)
```

where LME0 is the null model containing only random effects, LME1 includes `MovType` as fixed factor, and LME2 is the model that we formulated originally, which includes `MovType:Speed` (i.e. speed levels of passive movement) as fixed effect. The likelihood ratio test is done separately for each type of SMR (i.e. mu, beta ERD or beta rebound) at a given hemisphere, giving us a total of six p-values for each pair of models. Therefore, within each pair of models, we correct for multiple comparisons the six p-values using the false discovery rate (FDR). The significance level (critical alpha) in the statistical analysis is 0.05.

Then, only in the hemisphere and type of SMR (i.e. mu, beta ERD or beta rebound) that exhibits a significant difference between LME2 and LME1, we compute the pairwise differences between Least Squares Means [46] across different conditions, and we adjust for multiple comparisons by the FDR method.

TABLE I
P-VALUES OF THE LIKELIHOOD RATIO TESTS

A. Contralateral

Pair	mu band	beta band	beta rebound
LME0 - LME1	0.201	0.208	0.969
LME0 - LME2	0.658	0.257	**0.028**
LME1 - LME2	0.897	0.471	**0.025**

B. Ipsilateral

Pair	mu band	beta band	beta rebound
LME0 - LME1	**0.002**	**0.002**	0.224
LME0 - LME2	**0.001**	**0.041**	0.117
LME1 - LME2	**0.038**	0.897	0.172

For completeness, we evaluate whether, even if somewhere (e.g. contralateral mu ERD) a proportional relationship between `MovType:Speed` and the amplitude of SMR was not found, at least a non-zero constant relationship exists. For this purpose, we compute the significance of the Least Squares Means of each `MovType:Speed` condition against zero [46].

In the following two paragraphs, we describe how to interpret the statistical analysis pipeline, in order to facilitate the reading of the results section.

The LME0 - LME1 likelihood ratio test tells us whether the movement type (i.e. passive or active movement) contributes to model SMR activity better. Which can be interpreted as having a significantly different level of SMR between the two movement types. While, the LME1 - LME2 likelihood ratio test is to evaluate whether the addition of `MovType:Speed` improves the model likelihood. This can be interpreted as having significantly different SMR levels in some of the `MovType:Speed` levels. At this point, we still don't know specifically which levels are different, therefore we will have to analyse the pairwise differences between Least Squares Means. The LME0 - LME2 likelihood ratio test is simply done to confirm the effect of the combination of the two variables (i.e. `MovType` and `MovType:Speed`) over the null model (see Table I for the results).

The pairwise differences between Least Squares Means tell us specifically which pairs of `MovType:Speed` levels are significantly different from each other. Then, by looking at the *Estimate* column of Table II and at Fig. 3 we can tell the direction of the differences. Therefore, if we observe that the *Estimate* of differences among speed levels are significantly negative (i.e. the rightmost element of the difference is larger) or positive (i.e. the rightmost is smaller), we can conclude that there is a directly or inversely proportional relationship, respectively.

III. RESULTS

The boxplots showing both hemispheres' ERD/ERS magnitudes, across movement types and speeds, are visualized in Fig. 3. The results of the likelihood ratio test after multiple comparison correction among the three models LME0, LME1, LME2 are shown in Table I.

The main finding of this study is that contralateral beta rebound and ipsilateral mu ERD amplitudes are proportional to passive movement speed. Indeed, we observe that in

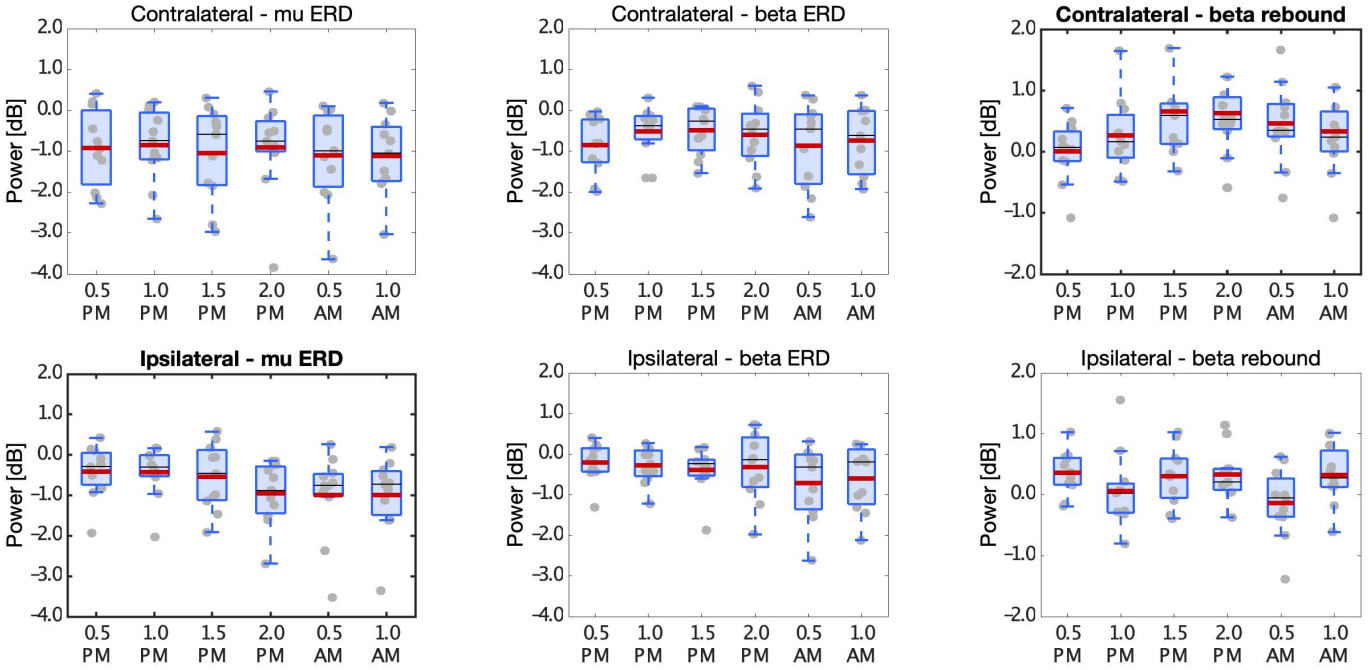

Fig. 3. Boxplots representing the relationship between experimental conditions and sensorimotor power amplitude for each hemisphere and type of SMR (i.e. mu, beta ERD and beta rebound). Contralateral beta rebound and ipsilateral mu ERD are highlighted in bold, since they are the ones exhibiting a significant effect of passive movement speed. Within each boxplot the mean is represented in red, and the median in black. Each dot represents one subject.

the last column of Table IA and in the first column of Table IB, LME2 is significantly different from LME1 and LME0, indicating that `MovType:Speed` has a main effect on contralateral beta rebound and ipsilateral mu ERD, respectively. This effect can be observed in Fig. 3, in the panels titled *contralateral beta rebound* and *ipsilateral mu ERD*. We see that, with respect to the baseline power, contralateral beta rebound power increases and ipsilateral mu ERD power decreases proportionally to passive movement speed.

Table II shows the result of subsequent post-hoc multiple comparisons between speed levels. It was computed only for those types of SMR and hemispheres that showed a significant effect of `MovType:Speed` in the likelihood ratio test (i.e. contralateral beta rebound and ipsilateral mu ERD). With respect to the contralateral beta rebound, we observe that PM0.5 is significantly ($p < 0.05$) different from PM1.5, PM2.0, AM0.5. In the ipsilateral mu ERD, the lower passive speeds (i.e. PM0.5, PM1.0 and PM1.5) are significantly different from PM2.0 and from the active movements.

Another important finding is that contralateral mu and beta ERD have a non-zero constant relationship with movement types and speed. In other words, contralateral mu and beta ERD are strong during any type of motion, equally across speed levels and movement types. This is evidenced by the results of the Least Squares Means analysis of each `MovType:Speed` condition against zero. Indeed, in the contralateral mu and beta ERD, all the conditions across speed and movement types are significantly different ($p < 0.05$) from zero (see Fig. 3). Moreover, `MovType` and `MovType:Speed` have no effect on the contralateral mu and beta ERD as indicated by the likelihood ratio test in Table IA, showing that the three models LME0, LME1, LME2 are not different from each other in the first two columns. This non-zero constant relationship is also visible in Fig. 3, where the contralateral mu and beta ERD do not vary with respect to movement type or speed, but lie on a constant level of -0.99 ± 0.11 db and -0.68 ± 0.17 db, respectively.

We also observe that ipsilateral mu and beta ERD levels are stronger in active than in passive movements. Indeed, in the first two columns of Table IB, LME1 is significantly different from LME0, indicating that `MovType` has a main factor on ipsilateral mu and beta ERD. However, LME2 and LME1 are not different from each other in the second column of Table IB, suggesting that `MovType:Speed` does not add any benefit to the modeling of the ipsilateral beta ERD. Moreover, LME1 is not significantly different from LME0 in the last column of Table IA, indicating `MovType` alone is not enough to explain the contralateral beta rebound.

IV. Discussion

We found that contralateral beta rebound and ipsilateral mu ERD amplitudes are proportional to passive movement speed; that contralateral mu and beta ERD are strong during any type of motion, equally across speed levels and movement types; and that ipsilateral mu and beta ERD levels are stronger in active than in passive movements.

Previous literature [24] hypothesized that the contralateral beta rebound may reflect post-movement inhibition proportional to the preceding activation of the motor area, meaning that contralateral activity is proportional to speed during passive movement. However, contralateral mu and beta ERD, though strong, have a constant relationship with speed. This

TABLE II
PAIRWISE COMPARISONS OF SPEED LEVELS

	Contralateral - beta rebound		
	Estimate	t-value	p-value
PM:0.5 - PM:1.0	-0.3	-1.35	0.368
PM:0.5 - PM:1.5	-0.7	-3.36	**0.004**
PM:0.5 - PM:2.0	-0.6	-3.22	**0.003**
PM:0.5 - AM:0.5	-0.5	-2.35	**0.023**
PM:0.5 - AM:1.0	-0.3	-1.67	0.100
PM:1.0 - PM:1.5	-0.4	-2.02	0.098
PM:1.0 - PM:2.0	-0.4	-1.87	0.067
PM:1.0 - AM:0.5	-0.2	-1.00	0.324
PM:1.0 - AM:1.0	-0.1	-0.33	0.746
PM:1.5 - PM:2.0	0.0	0.14	0.887
PM:1.5 - AM:0.5	0.2	1.02	0.313
PM:1.5 - AM:1.0	0.3	1.69	0.097
PM:2.0 - AM:0.5	0.2	0.88	0.770
PM:2.0 - AM:1.0	0.3	1.55	0.256
AM:0.5 - AM:1.0	0.1	0.75	0.979

	Ipsilateral - mu ERD		
	Estimate	t-value	p-value
PM:0.5 - PM:1.0	0.0	0.08	0.940
PM:0.5 - PM:1.5	0.1	0.77	0.443
PM:0.5 - PM:2.0	0.5	3.15	**0.003**
PM:0.5 - AM:0.5	0.6	3.39	**0.002**
PM:0.5 - AM:1.0	0.6	3.36	**0.004**
PM:1.0 - PM:1.5	0.1	0.7	0.488
PM:1.0 - PM:2.0	0.5	3.07	**0.006**
PM:1.0 - AM:0.5	0.6	3.31	**0.004**
PM:1.0 - AM:1.0	0.6	3.28	**0.004**
PM:1.5 - PM:2.0	0.4	2.37	**0.042**
PM:1.5 - AM:0.5	0.4	2.61	**0.024**
PM:1.5 - AM:1.0	0.4	2.59	**0.026**
PM:2.0 - AM:0.5	0.0	0.24	0.812
PM:2.0 - AM:1.0	0.0	0.21	0.832
AM:0.5 - AM:1.0	0.0	-0.03	0.979

is congruent with earlier studies showing that the power of contralateral beta rebound, but not contralateral ERD, depends on active movement speed [26], [27]. Parkkonen *et al.* [22] found that contralateral beta rebound was stronger in passive movements than in tactile stimulation. They hypothesized that the rebound magnitude depends on the type and quantity of afferent input, and that the larger beta rebound of a passive movement indicates a stronger interaction with motor output for proprioceptive afferents than tactile ones. This is in line with other studies about active movements that found contralateral beta rebound differences between index and four-finger flexion [47], brief ballistic wrist movement and sustained isometric wrist extension [18], different types of ballistic movements [48] and different levels of activated muscle mass [49]. Moreover, voluntary movement and mixed-nerve stimulation elicit a stronger rebound than pure tactile stimulation [32]. Interestingly, only one study found a proportional relationship between contralateral ERD and active hand clenching speed [28]. All in all, our results suggest that faster passive movements produce a larger amount of afferent input, which is reflected in the proportional contralateral beta rebound.

With respect to ipsilateral mu ERD, its amplitude increases with speed. This finding is consistent with the hypothesis that ipsilateral activity is proportional to active movement speed, and that it represents speed-dependent inhibitory processes: increased ipsilateral inhibitory activity is associated with the neural processes of stopping faster movements [50]. Moreover, transcallosal inhibitory signals contribute to the suppression of unintended movements [50]–[52]. Based on the cited literature, we speculate that a faster passive movement elicits a stronger ipsilateral activation, associated with the inhibitory signals triggered by an involuntary movement.

The active movement condition was included in the experiment to serve as a control with respect to the excitability during the active condition of each subject's SMR. We found that the ERD power during active movements is significantly larger than that of passive movements in ipsilateral mu and beta ERD. Moreover, the post-hoc pairwise comparison shows that active movements have a stronger contralateral beta rebound compared to the slowest passive movement (i.e. PM0.5). These results are in agreement with previous studies showing that ipsilateral ERD [53] and contralateral beta rebound [17] are weaker in passive movements than in active ones, especially when the speed of the movement is equivalent [21].

As opposed to the results of [28], no significant difference was found between the SMR amplitude of the two active movement speed conditions. This may be due to the limited levels of active movment speed that were investigated, or to the fact that forearm oscillations have different SMR patterns compared to hand clenching [49].

Seeber *et al.* [54] found two types of spatially overlapping large-scale networks in an rhythmic active finger tapping EEG experiment: a sustained ERD that represents finger movement, and superimposed phase-related amplitudes that resemble the flexion and extension sequence of the fingers. In our data, we could not find such time-dependent modulation in the time-frequency representation of the sensorimotor independent components, neither in the active nor in the passive movement conditions. Indeed, in our data we observe a typical ERD and post-movement rebound (i.e. discrete activation), rather than continuously modulated sensorimotor rhythms such as the one found in Seeber *et al.* [54]. This may be due to the fact that the duration of our motor task was too short or to the different pathways associated with attention and control of gross elbow movements.

By comparing the biceps muscle activity (i.e. EMG) across conditions, we confirmed that subjects did not inadvertently produce voluntary muscle contractions during passive movements. Moreover, it is unlikely that the results are caused by muscle or mechanical artifacts, considering that only specific hemispheres, frequency bands and time periods are proportional to speed, while others display a constant relationship.

In the present study, the motor task was executed on the non-dominant hand of right handed subjects. This was done to consider a larger population while minimizing experimental conditions. Therefore, the generality of our findings should be confirmed in future works. Previously, an EEG study of finger movement handedness has shown that only pre-movement SMR are affected by handedness [55]. However, fine motor control of finger movements uses different pathways than gross motor control of elbow movements. Therefore, in future, the effect of hand dominance on the sensorimotor rhythms during passive movements should be investigated.

It should be noted that the linear mixed effects model LME2 includes speed only as a nested variable within movement type. As a result, the model does not allow to evaluate the full interaction between speed and movement type.

The findings of our study could be relevant for the proprioceptive neurofeedback and motor rehabilitation communities. Indeed, it has been suggested that beta rebound correlates with motor recovery after stroke [56]. The beta rebound could be monitored under several speed levels, in order to assess cortical excitability after stroke [22]. Moreover, novel rehabilitation procedures may be introduced, where the intensity of proprioceptive input is programmed to switch between different levels, and the brain activity is fed back visually to the subjects with the goal of achieving a proportional SMR power.

V. Conclusion

Our results revealed three functionally distinct frequency-specific neuronal populations with respect to passive movements. Contralateral mu and beta ERD have a strong but constant relationship with passive movement speed, which reveals an all-or-nothing type of activation in the motor cortex. In the same hemisphere (i.e. contralateral), the proportional relationship between passive speed and beta rebound may be associated with the modulatory effect of afferent input quantity on motor cortex activity. In the ipsilateral hemisphere we found yet another frequency specific activity (i.e. mu ERD), proportional to speed, that has been previously related to speed-dependent inhibitory processes.

References

[1] L. Masia, M. Xiloyannis, D. B. Khanh, A. C. Wilson, S. Contu, and K. G. Yongtae, "Actuation for robot-aided rehabilitation: Design and control strategies," in *Rehabilitation Robotics*, R. Colombo and V. Sanguineti, Eds. New York, NY, USA: Academic, 2018, ch. 4, pp. 47–61.

[2] A. Turolla, "An overall framework for neurorehabilitation robotics: Implications for recovery," in *Rehabilitation Robotics*, R. Colombo and V. Sanguineti, Eds. New York, NY, USA: Academic, 2018, ch. 2, pp. 15–27.

[3] K. Shindo *et al.*, "Effects of neurofeedback training with an electroencephalogram-based brain-computer interface for hand paralysis in patients with chronic stroke: A preliminary case series study," *J. Rehabil. Med.*, vol. 43, no. 10, pp. 951–957, 2011.

[4] A. Ramos-Murguialday *et al.*, "Brain-machine interface in chronic stroke rehabilitation: A controlled study," *Ann. Neurol.*, vol. 74, no. 1, pp. 100–108, 2013.

[5] T. Ono *et al.*, "Brain-computer interface with somatosensory feedback improves functional recovery from severe hemiplegia due to chronic stroke," *Front. Neuroeng.*, vol. 7, p. 19, Jul. 2014.

[6] K. C. Elliott, D. T. Bundy, D. J. Guggenmos, and R. J. Nudo, "Physiological basis of neuromotor recovery," in *Rehabilitation Robotics*, R. Colombo and V. Sanguineti, Eds. New York, NY, USA: Academic, 2018, ch. 1, pp. 1–13.

[7] S. Silvoni *et al.*, "Brain-computer interface in stroke: A review of progress," *Clin. EEG Neurosci.*, vol. 42, no. 4, pp. 245–252, 2011.

[8] G. Lisi and J. Morimoto, "Noninvasive brain machine interfaces for assistive and rehabilitation robotics: A review," in *Human Modelling for Bio-Inspired Robotics*. Cambridge, MA, USA: Academic, 2016, pp. 187–216.

[9] E. Kandel, J. Schwartz, and T. Jessell, *Principles of Neural Science*, vol. 4. New York, NY, USA: McGraw-Hill, 2000.

[10] K. P. Blum, B. L. D'Incamps, D. Zytnicki, and L. H. Ting, "Force encoding in muscle spindles during stretch of passive muscle," *PLOS Comput. Biol.*, vol. 13, no. 9, Sep. 2017, Art. no. e1005767. doi: 10.1371/journal.pcbi.1005767.

[11] P. B. C. Matthews, "The response of de-efferented muscle spindle receptors to stretching at different velocities," *J. Physiol.*, vol. 168, no. 3, pp. 660–678, 1963.

[12] H. Asanuma, K. Larsen, and H. Yumiya, "Peripheral input pathways to the monkey motor cortex," *Experim. Brain Res.*, vol. 38, no. 3, pp. 349–355, Feb. 1980.

[13] D. P. Friedman and E. G. Jones, "Thalamic input to areas 3a and 2 in monkeys," *J. Neurophysiol.*, vol. 45, no. 1, pp. 59–85, 1981.

[14] E. G. Jones and S. P. Wise, "Size, laminar and columnar distribution of efferent cells in the sensory-motor cortex of monkeys," *J. Comparative Neurol.*, vol. 175, no. 4, pp. 391–437, 1977.

[15] E. G. Jones, J. D. Coulter, and S. H. Hendry, "Intracortical connectivity of architectonic fields in the somatic sensory, motor and parietal cortex of monkeys," *J. Comparative Neurol.*, vol. 181, no. 2, pp. 291–347, 1978.

[16] E. G. Jones, "The nature of the afferent pathways conveying short-latency inputs to primate motor cortex," *Adv. Neurol.*, vol. 39, pp. 263–285, Jan. 1983.

[17] F. Cassim *et al.*, "Does post-movement beta synchronization reflect an idling motor cortex?" *Neuroreport*, vol. 12, no. 17, pp. 3859–3863, Dec. 2001.

[18] M. Alegre, A. Labarga, I. G. Gurtubay, J. Iriarte, A. Malanda, and J. Artieda, "Beta electroencephalograph changes during passive movements: Sensory afferences contribute to beta event-related desynchronization in humans," *Neurosci. Lett.*, vol. 331, no. 1, pp. 29–32, 2002.

[19] G. R. Müller, C. Neuper, R. Rupp, C. Keinrath, H. J. Gerner, and G. Pfurtscheller, "Event-related beta EEG changes during wrist movements induced by functional electrical stimulation of forearm muscles in man," *Neurosci. Lett.*, vol. 340, no. 2, pp. 143–147, Apr. 2003.

[20] S. D. Muthukumaraswamy, "Functional properties of human primary motor cortex gamma oscillations," *J. Neurophysiol.*, vol. 104, no. 5, pp. 2873–2885, Nov. 2010.

[21] D. O. Cheyne, "MEG studies of sensorimotor rhythms: A review," *Exp. Neurol.*, vol. 245, pp. 27–39, Jul. 2013.

[22] E. Parkkonen, K. Laaksonen, H. Piitulainen, L. Parkkonen, and N. Forss, "Modulation of the ~20-Hz motor-cortex rhythm to passive movement and tactile stimulation," *Brain Behav.*, vol. 5, no. 5, 2015, Art. no. e00328.

[23] G. Pfurtscheller, "Functional brain imaging based on ERD/ERS," *Vis. Res.*, vol. 41, nos. 10–11, pp. 1257–1260, 2001.

[24] G. Pfurtscheller and F. H. L. da Silva, "Event-related EEG/MEG synchronization and desynchronization: Basic principles," *Clin. Neurophysiol.*, vol. 110, pp. 1842–1857, Nov. 1999.

[25] G. Lisi, D. Rivela, A. Takai, and J. Morimoto, "Markov switching model for quick detection of event related desynchronization in EEG," *Frontiers Neurosci.*, vol. 12, p. 24, Feb. 2018.

[26] A. Stancák and G. Pfurtscheller, "Desynchronization and recovery of beta rhythms during brisk and slow self-paced finger movements in man," *Neurosci. Lett.*, vol. 196, nos. 1–2, pp. 21–24, Aug. 1995.

[27] A. Stancák and G. Pfurtscheller, "Event-related desynchronisation of central beta-rhythms during brisk and slow self-paced finger movements of dominant and nondominant hand," *Brain Res. Cognit. Brain Res.*, vol. 4, no. 3, pp. 171–183, Oct. 1996.

[28] H. Yuan, C. Perdoni, and B. He, "Relationship between speed and EEG activity during imagined and executed hand movements," *J. Neural Eng.*, vol. 7, no. 2, 2010, Art. no. 026001.

[29] G. R. Müller-Putz, D. Zimmermann, B. Graimann, K. Nestinger, G. Korisek, and G. Pfurtscheller, "Event-related beta EEG-changes during passive and attempted foot movements in paraplegic patients," *Brain Res.*, vol. 1137, no. 1, pp. 84–91, 2007.

[30] G. Lisi, T. Noda, and J. Morimoto, "Decoding the ERD/ERS: Influence of afferent input induced by a leg assistive robot," *Frontiers Syst. Neurosci.*, vol. 8, p. 85, May 2014.

[31] A. C. Sittig, J. J. D. van der Gon, and C. C. Gielen, "The contribution of afferent information on position and velocity to the control of slow and fast human forearm movements," *Exp. Brain Res.*, vol. 67, no. 1, pp. 33–40, 1987.

[32] E. Houdayer, E. Labyt, F. Cassim, J. L. Bourriez, and P. Derambure, "Relationship between event-related beta synchronization and afferent inputs: Analysis of finger movement and peripheral nerve stimulations," *Clin. Neurophysiol.*, vol. 117, no. 3, pp. 628–636, Mar. 2006.

[33] A. Stancák, J. Svoboda, R. Rachmanová, J. Vrána, J. Králík, and J. Tintera, "Desynchronization of cortical rhythms following cutaneous stimulation: Effects of stimulus repetition and intensity, and of the size of corpus callosum," *Clin. Neurophysiol.*, vol. 114, no. 10, pp. 1936–1947, 2003.

[34] T. Teramae, T. Noda, S.-H. Hyon, and J. Morimoto, "Modeling and control of a pneumatic-electric hybrid system," in *Proc. IEEE/RSJ Int. Conf. Intell. Robots Syst.*, Nov. 2013, pp. 4887–4892.

[35] G. Lisi, M. Hamaya, T. Noda, and J. Morimoto, "Dry-wireless EEG and asynchronous adaptive feature extraction towards a plug-and-play co-adaptive brain robot interface," in *Proc. IEEE Int. Conf. Robot. Autom. (ICRA)*, May 2016, pp. 959–966.

[36] N. C. Chesler and W. K. Durfee, "Surface EMG as a fatigue indicator during FES-induced isometric muscle contractions," *J. Electromyogr. Kinesiol.*, vol. 7, no. 1, pp. 27–37, 1997.

[37] T. Mullen *et al.*, "Real-time modeling and 3D visualization of source dynamics and connectivity using wearable EEG," in *Proc. 35th Annu. Int. Conf. IEEE Eng. Med. Biol. Soc. (EMBC)*, Jul. 2013, pp. 2184–2187.

[38] A. Delorme, T. Sejnowski, and S. Makeig, "Enhanced detection of artifacts in EEG data using higher-order statistics and independent component analysis," *NeuroImage*, vol. 34, no. 4, pp. 1443–1449, 2007.

[39] J. A. Palmer, K. Kreutz-Delgado, and S. Makeig, "AMICA: An adaptive mixture of independent component analyzers with shared components," Swartz Center Computatonal Neursosci., Univ. California San Diego, San Diego, CA, USA, Tech. Rep., 2011.

[40] Y. Wang, Y.-T. Wang, and T.-P. Jung, "Translation of EEG spatial filters from resting to motor imagery using independent component analysis," *PLoS ONE*, vol. 7, no. 5, May 2012, Art. no. e37665.

[41] A. Delorme and S. Makeig, "EEGLAB: An open source toolbox for analysis of single-trial EEG dynamics including independent component analysis," *J. Neurosci. Methods*, vol. 134, no. 1, pp. 9–21, Mar. 2004.

[42] S. D. Muthukumaraswamy, "High-frequency brain activity and muscle artifacts in MEG/EEG: A review and recommendations," *Frontiers Hum. Neurosci.*, vol. 7, p. 138, Apr. 2013.

[43] G. Lisi and J. Morimoto, "EEG single-trial detection of gait speed changes during treadmill walk," *PLoS ONE*, vol. 10, no. 5, May 2015, Art. no. e0125479.

[44] R. Grandchamp and A. Delorme, "Single-trial normalization for event-related spectral decomposition reduces sensitivity to noisy trials," *Frontiers Psychol.*, vol. 2, p. 236, Sep. 2011.

[45] B. Blankertz, R. Tomioka, S. Lemm, M. Kawanabe, and K. R. Müller, "Optimizing spatial filters for robust EEG single-trial analysis," *IEEE Signal Process. Mag.*, vol. 25, no. 1, pp. 41–56, Jan. 2008.

[46] A. Kuznetsova, P. B. Brockhoff, and R. H. B. Christensen, "LmerTest package: Tests in linear mixed effects models," *J. Stat. Softw.*, vol. 82, no. 13, pp. 1–26, 2017.

[47] R. Salmelin, N. Forss, J. Knuutila, and R. Hari, "Bilateral activation of the human somatomotor cortex by distal hand movements," *Electroencephalogr. Clin. Neurophysiol.*, vol. 95, no. 6, pp. 444–452, Dec. 1995.

[48] L. Wheaton, E. Fridman, S. Bohlhalter, S. Vorbach, and M. Hallett, "Left parietal activation related to planning, executing and suppressing praxis hand movements," *Clin. Neurophysiol.*, vol. 120, no. 5, pp. 980–986, May 2009.

[49] G. Pfurtscheller, K. Zalaudek, and C. Neuper, "Event-related beta synchronization after wrist, finger and thumb movement," *Electroencephalogr. Clin. Neurophysiol./Electromyogr. Motor Control*, vol. 109, no. 2, pp. 154–160, Apr. 1998.

[50] T. Tazoe and M. A. Perez, "Speed-dependent contribution of callosal pathways to ipsilateral movements," *J. Neurosci.*, vol. 33, no. 41, pp. 16178–16188, Oct. 2013.

[51] M. Cincotta and U. Ziemann, "Neurophysiology of unimanual motor control and mirror movements," *Clin. Neurophysiol.*, vol. 119, no. 4, pp. 744–762, Apr. 2008.

[52] F. Giovannelli *et al.*, "Modulation of interhemispheric inhibition by volitional motor activity: An ipsilateral silent period study," *J. Physiol.*, vol. 587, pp. 5393–5410, Nov. 2009.

[53] E. Formaggio *et al.*, "Modulation of event-related desynchronization in robot-assisted hand performance: Brain oscillatory changes in active, passive and imagined movements," *J. Neuroeng. Rehabil.*, vol. 10, no. 1, p. 24, Feb. 2013.

[54] M. Seeber, R. Scherer, and G. R. Müller-Putz, "EEG oscillations are modulated in different behavior-related networks during rhythmic finger movements," *J. Neurosci.*, vol. 36, no. 46, p. 11671–11681, 2016.

[55] A. Stancák, Jr., and G. Pfurtscheller, "The effects of handedness and type of movement on the contralateral preponderance of μ-rhythm desynchronisation," *Electroencephalogr. Clin. Neurophysiol.*, vol. 99, no. 2, pp. 174–182, 1996.

[56] K. Laaksonen *et al.*, "Effect of afferent input on motor cortex excitability during stroke recovery," *Clin. Neurophysiol.*, vol. 123, no. 12, pp. 2429–2436, 2012.